Biochimica et Biophysica Acta 1853 (2015) 2251–2260

Contents lists available at ScienceDirect

Biochimica et Biophysica Acta

journal homepage: www.elsevier.com/locate/bbamcr

Biphasic effect of PTK7 on KDR activity in endothelial cells and angiogenesis

Won-Sik Shin, Hye-Won Na, Seung-Taek Lee *

Department of Biochemistry, College of Life Science and Biotechnology, Yonsei University, Seoul, Republic of Korea

ARTICLE INFO

Article history:
Received 10 February 2015
Received in revised form 27 April 2015
Accepted 5 May 2015
Available online 16 May 2015

Keywords:
Defective receptor protein tyrosine kinase
PTK7
KDR
VEGF
Angiogenesis

ABSTRACT

Protein tyrosine kinase 7 (PTK7) is a member of the defective receptor protein tyrosine kinase family which lacks catalytic activity. Expression of PTK7 is increased in various cancers but its role in carcinogenesis is not well understood. We previously showed that disruption of PTK7 function suppresses VEGF-induced angiogenic phenotypes in HUVECs and mice. Here, we investigated molecular mechanisms for modulating VEGF-induced physiological effects by PTK7. Treatment with a high concentration of extracellular domain of PTK7 (soluble PTK7; sPTK7) or knockdown of PTK7 inhibited VEGF-induced phosphorylation of kinase insert domain receptor (KDR) but did not inhibit phosphorylation of fms-related tyrosine kinase 1 (FLT-1) in HUVECs. PTK7, more specifically sPTK7, interacted with KDR but not with FLT-1 in HUVECs and HEK293 cells. *In vitro* binding assay showed that sPTK7 formed oligomers with the extracellular domain of KDR (sKDR) up to an approximately 1:3 molar ratio, and *vice versa*. sPTK7 at lower molar ratios than sKDR enhanced the binding of VEGF to sKDR. At the same or higher molar ratios, it reduced the binding of VEGF to sKDR. Increasing concentrations of sPTK7 or increasing levels of PTK7 expression first increased and then decreased VEGF-induced KDR phosphorylation, migration, and capillary-like tube formation of HUVECs, as well as *in vivo* angiogenesis. Taken together, our data demonstrates that PTK7 regulates the activity of KDR biphasically by inducing oligomerization of KDR molecules at lower concentrations and by surrounding KDR molecules at higher concentrations.

1. Introduction

A subgroup of receptor protein tyrosine kinases (RPTKs) is defective in tyrosine kinase activity because of alterations in motifs important for catalytic activity [1]. Such defective RPTKs include protein tyrosine kinase 7 (PTK7), HER3 (ErbB3), EphA10, EphB6, and Ryk. Despite their lack of kinase activity, some of these defective RPTKs are known to promote signal transduction by interacting with other proteins. For example, HER3 bound to neuregulin forms heterodimers with other EGFR family members and activates downstream signals, such as PI3-kinase and MAP kinases [2,3]. Ryk interacts with Eph receptors, EphB2 and EphB3, and regulates cell migration during craniofacial and cortical development [4–6]. Ryk also functions as a co-receptor for Wnt signal molecules and modulates Wnt signaling pathways during neural development [7,8].

PTK7, also known as colon carcinoma kinase 4 (CCK-4), is composed of an extracellular domain with seven immunoglobulin-like loops, a transmembrane domain, and a defective tyrosine kinase domain [9–12]. *Drosophila* Dtrk/OTK and chick KLG, which are likely orthologues of human PTK7, contribute to repulsive axon guidance in *Drosophila* development and ventricle segment formation during chick cardiac morphogenesis through interaction with plexins, which are receptors for semaphorins [13,14]. Mammalian PTK7 is known to regulate planar cell polarity (PCP) signaling, based on the finding that mice homozygous for a truncated PTK7 gene were perinatally lethal, with failure of neural closure and misorientation of the stereociliary bundle [15]. Recently it was reported that PTK7 also regulates canonical and non-canonical Wnt signaling pathways [16,17].

PTK7 expression is elevated in various cancers, including esophageal squamous cell carcinoma and colon cancer [18–20]. Conversely, its expression is decreased in other cancers such as metastatic melanoma and ovarian carcinoma [21,22]. These findings suggest that its expression level is not directly related to tumorigenesis. Interestingly, we previously found that PTK7 is shed by ADAM17 and further cleaved by γ-secretase in colon cancer cells [23]. The cleaved PTK7 cytosolic domain translocates from plasma membrane to the nucleus and enhances tumorigenesis.

PTK7 mRNA levels are modulated during vascular endothelial growth factor (VEGF)-induced capillary-like tube formation by human umbilical vein endothelial cells (HUVECs) [24]. Functional disruption of PTK7 by treatment with the PTK7 extracellular domain (soluble PTK7; sPTK7) as a decoy receptor or knockdown of PTK7 decreased

Abbreviations: FLT-1, fms-related tyrosine kinase 1; HUVEC, human umbilical vein endothelial cell; KDR, kinase insert domain receptor; PTK7, protein tyrosine kinase 7; RPTK, receptor protein tyrosine kinase; VEGF, vascular endothelial growth factor.

* Corresponding author at: Department of Biochemistry, College of Life Science and Biotechnology, Yonsei University, Seoul 120-749, Republic of Korea. Tel.: +82 2 2123 2703; fax: +82 2 362 9897.

E-mail address: stlee@yonsei.ac.kr (S.-T. Lee).

http://dx.doi.org/10.1016/j.bbamcr.2015.05.015
0167-4889/

VEGF-induced migration, invasion, and tube-formation of HUVECs, and angiogenesis *in vivo* [24]. Therefore, PTK7 at the plasma membrane probably plays an important role in VEGF-mediated signaling. To further understand the effect of PTK7 on signaling pathways induced by VEGF, we identified molecules interacting with PTK7. We then analyzed the changes in the activity of PTK7-interacting proteins upon exposure to different PTK7 levels, as well as the effects of different PTK7 levels on migration and tube-formation by HUVECs, and on angiogenesis *in vivo*. Based on the results, we propose a model for the action of PTK7.

2. Materials and methods

2.1. Antibodies

The following antibodies were used: anti-FLT-1, anti-phospho-Erk, anti-Erk, anti-p38, anti-VEGF, and anti-β-actin antibodies from Santa Cruz Biotechnology (Santa Cruz, CA, USA); anti-phospho-KDR (Y951), anti-KDR, anti-phospho-p38, anti-phospho-Akt (S473), anti-Akt, anti-phospho-eNOS (S1177), anti-eNOS, anti-phospho-JNK, and anti-JNK antibodies from Cell Signaling Technology (Beverly, MA, USA); anti-phospho-tyrosine (clone 4G10) antibody from Upstate (Lake Placid, NY, USA); anti-FLAG-M2 antibody from Sigma-Aldrich (St. Louis, MO, USA); anti-penta-His antibody from Qiagen (Cambridge, MA, USA); anti-phospho-FLT-1 (Y1213) antibody from R&D Systems (Minneapolis, MN, USA), and horseradish peroxidase-conjugated goat anti-mouse-IgG, anti-rabbit-IgG or anti-human-Fc antibodies from KOMA Biotech (Seoul, Korea). Rabbit anti-PTK7 anti-serum was described previously [24].

2.2. Cell culture

HUVECs were grown in M199 medium supplemented with 20% FBS (Hyclone, South Logan, UT, USA), 5 U/ml heparin, and 3 ng/ml bFGF (Upstate) and were used in passages 5–8. Human embryonic kidney (HEK) 293 cell lines were grown in DMEM supplemented with 10% bovine serum, 100 U/ml penicillin, and 100 μg/ml streptomycin. All cells were grown at 37 °C in 5% CO_2.

2.3. Expression and knockdown vectors

pRSET-A-KDR harboring human full-length kinase insert domain receptor (KDR; VEGF receptor 2) cDNA and pCI-Neo-FLT-1 encoding human fms-related tyrosine kinase 1 (FLT-1; VEGF receptor 1) were a kind gift from Dr. Yong Song Gho (POSTECH, Korea). pcDNA3-sKDR-Fc and pcDNA3-sFLT-1-Fc encoding the extracellular domain of KDR (amino acids 1–764) and FLT-1 (amino acids 1–687) with a C-terminal Fc fragment, respectively, were generous gifts from Dr. Gou Young Koh (KAIST, Korea). Construction of the following expression vectors is described in the Supplementary materials: pcDNA3-hPTK7-FLAG encoding human PTK7 with a C-terminal Flag tag, pcDNA3-PTK7-TM-Cyt-FLAG encoding transmembrane and cytosolic domains of human PTK7 with a C-terminal Flag tag, and pcDNA3.1-Kozak-KDR encoding human KDR. Constructs pLKO.1-shRNA-PTK7-6433 and -6434 for human PTK7 knockdown vectors and pLKO.1-control (Sigma-Aldrich) were described previously [20].

2.4. Transfection of expression and knockdown vectors

For stable expression in HEK293 cells, subconfluent cells were transfected by the calcium phosphate method [25] and were grown in the presence of 1.2 mg/ml G418 for two weeks. G418-resistant colonies were isolated as individual clones or cultured as mixed populations. For transient expression in HEK293 cells, transfection was performed by the same procedures as for stable expression. For transient transfection into HUVECs, subconfluent cells were transfected using Lipofectamine 2000 (Invitrogen, Carlsbad, CA, USA) according to the manufacturer's instructions. Transfected cells were used two days after transfection.

2.5. Transfection of siRNA

siRNA mixture against human PTK7 was transfected into HUVECs as described previously [24].

2.6. Purification of sPTK7, sKDR, and sFLT-1

Purification of human and mouse sPTK7 with a C-terminal His tag (sPTK7-His) was previously described [24]. For purification of human sKDR and human sFLT-1 fused to a C-terminal Fc (sKDR-Fc and sFLT-1-Fc), stable clones expressing sKDR-Fc or sFLT-1-Fc were cultured in serum-free medium for seven days. The conditioned medium was subjected to ammonium sulfate precipitation with 70% saturation. The pellets were dissolved in 0.1 M Tris–HCl (pH 8.0) containing 1 mM PMSF and 1 mM EDTA. Protein-A Sepharose (Sigma-Aldrich) was added to the supernatant, washed with 0.1 M Tris–HCl (pH 8.0), and eluted with 0.1 M glycine–HCl (pH 3.0). The eluent containing sKDR-Fc was neutralized with 0.1 volume of 1 M Tris–HCl (pH 8.0) immediately and dialyzed against PBS [137 mM NaCl, 10 mM Na_2HPO_4, 2.7 mM KCl, 2 mM KH_2PO_4 (pH 7.4)] containing 1 mM PMSF.

2.7. Growth factor stimulation of HUVECs

Subconfluent HUVECs were serum-depleted in M199 medium supplemented with 1% FBS for 6 h. If necessary, the depleted cells were pre-incubated with the indicated proteins for 30 min. The cells were stimulated with 0.5 nM VEGF (KOMA Biotech), for 5 min for analysis of receptors, or for 10 min for analysis of other signaling molecules.

2.8. Immunoprecipitation, pull-down assays and immunoblotting

Cells were lysed with lysis buffer (50 mM Tris–HCl, pH 7.4, 150 mM NaCl, 1% NP-40) containing 5 mM NaF, 1 mM Na_3VO_4, and protease inhibitor cocktail III (Calbiochem, La Jolla, CA, USA). For immunoprecipitation, lysates were incubated with the indicated antibodies and protein-A/G agarose (Upstate) or mouse anti-FLAG M2-agarose. For pull-down assays, cell lysates and *in vitro* binding mixtures containing sPTK7-His, sKDR-Fc, or sFLT-1-Fc were incubated with Ni^{2+}-NTA agarose and protein-A Sepharose, respectively. The protein-bound resins were washed with lysis buffer or, in the case of the His-tag pull-down assay, with PBS containing 20 mM imidazole. For immunoblotting, cell lysates or immunoprecipitated or pulled-down proteins were resuspended in SDS-sample buffer, subjected to SDS-PAGE, and transferred to PVDF membranes. Immunoblotting was performed using the indicated antibodies, and immunoreactivity was visualized using Immobilon Western Chemiluminescent HRP Substrate (Millipore, Bedford, MA, USA) and a LAS-3000 imaging system (Fuji, Tokyo, Japan).

2.9. Chemotactic migration assay and capillary-like tube formation

These assays were performed as described previously [24] except that migration and tube formation assays were incubated for 4 h and 24 h, respectively.

2.10. Ethics statement

The protocol for animal studies was approved by the Institutional Animal Care and Use Committee of Yonsei University (Permit Number: 20130100). Animal studies were performed in accordance with the guidelines of the Committee.

2.11. In vivo Matrigel plug assay

Ice-cold Matrigel™ (BD Biosciences, Bedford, MA, USA) (0.25 ml) was mixed with 16 units of heparin, 2.5 nM mouse VEGF (KOMA

Biotech), and the indicated amounts of mouse sPTK7. The mixed Matrigel was injected subcutaneously into the abdomens of 7-week-old female C57BL/6 mice. After 9 days, the mice were killed, and the plugs were recovered. Blood vessel formation in the plugs was quantified by measurement of hemoglobin contents using a Drabkin reagent kit 525 (Sigma-Aldrich).

2.12. Statistical analysis

All data were based on at least three independent experiments and expressed as mean ± standard deviation. Statistical significance was analyzed by Student's *t*-test.

3. Results

3.1. Blocking endogenous PTK7 function inhibits VEGF-induced KDR activation

To examine the role of PTK7 in VEGF-induced signaling pathways in HUVECs, endogenous PTK7 function was counteracted by treatment with a high concentration of the purified sPTK7 (53 nM or 4 μg/ml, Supplementary Fig. 1) (Fig. 1A and Supplementary Fig. 2A) or knockdown of PTK7 (Fig. 1B and Supplementary Fig. 2B). Blocking PTK7 function inhibited VEGF-induced phosphorylation of KDR, Akt, eNOS, and ERK, but not the phosphorylation of FLT-1, JNK, and p38 MAPK. These results imply that PTK7 plays a role in the activation of KDR but not of FLT-1.

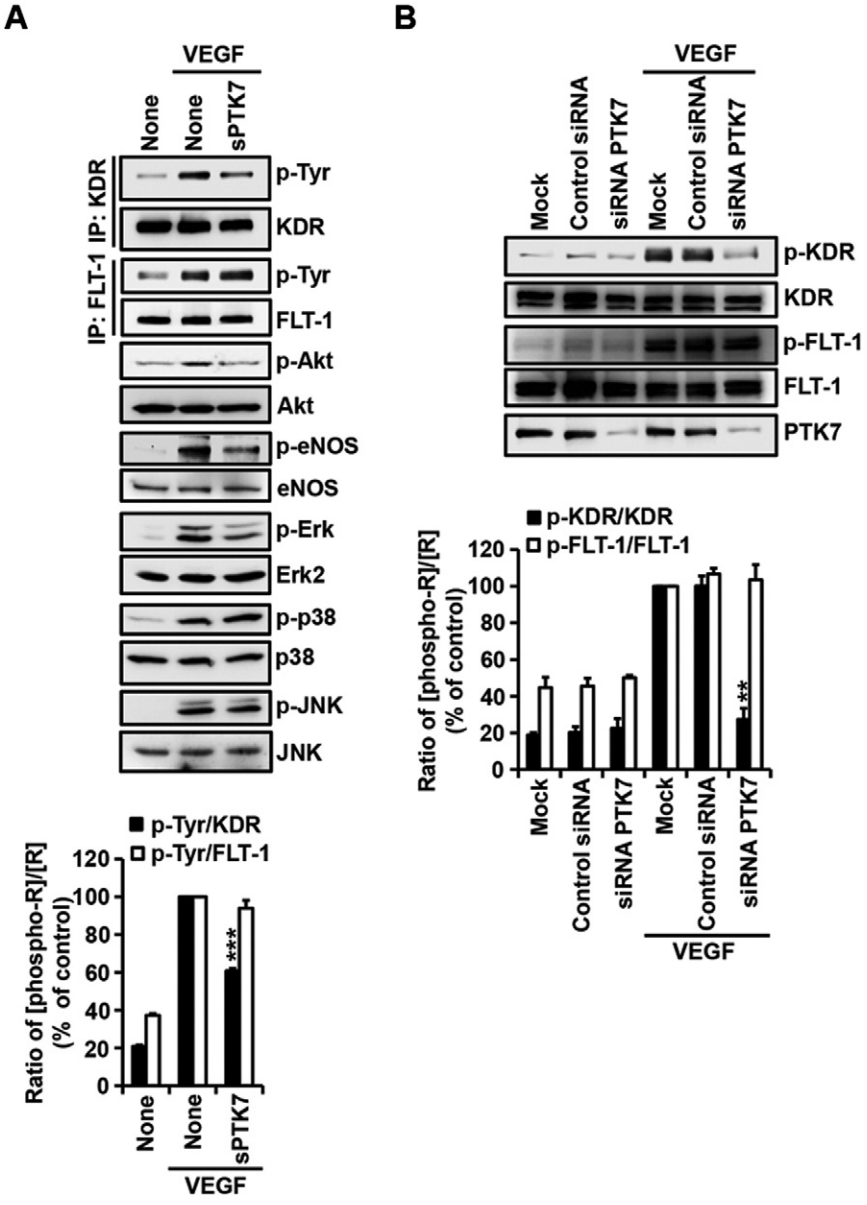

Fig. 1. Effect of sPTK7 or PTK7 knockdown on VEGF-induced phosphorylation of signaling molecules in HUVECs. (A) Subconfluent HUVECs were starved in M199 medium containing 1% FBS for 6 h and pretreated with 53 nM (4 μg/ml) sPTK7 for 30 min. (B) HUVECs in which PTK7 was silenced by transfection of siRNAs were starved in M199 medium supplemented with 1% FBS for 6 h. The cells were stimulated with 0.5 nM VEGF for 5 min to analyze phosphorylation of receptors or for 10 min to analyze phosphorylation of other signaling molecules. Phosphorylation levels of KDR and FLT-1 were analyzed by immunoprecipitation of cell lysates and immunoblotting using an anti-phospho-tyrosine antibody (A) or by immunoblot analysis with anti-phospho-KDR (Y951) and anti-phospho-FLT-1 (Y1213). Silencing of PTK7 and phosphorylation levels of other signaling molecules were examined by immunoblot analysis with anti-PTK7, anti-phospho-Akt (S473), anti-phospho-eNOS (S1177), anti-phospho-ERK, anti-phospho-p38, and anti-phospho-JNK antibodies. Representative data from three independent experiments are shown. Phosphorylation levels of VEGF receptors were estimated by densitometry. Graphs show the relative levels of receptor phosphorylation ([phospho-R]/[R]). $^{**}P < 0.01$ and $^{***}P < 0.001$ *vs.* a sample treated with VEGF alone.

3.2. The extracellular domain of PTK7 interacts with the extracellular domain of KDR

To understand how PTK7 increases phosphorylation of KDR, the interaction between PTK7 and VEGF receptors was analyzed by pull-down assays in HUVECs which endogenously express KDR and FLT-1 as well as PTK7. KDR was co-precipitated with PTK7 but FLT-1 was not (Fig. 2A left panel). After silencing of PTK7 in HUVECs, KDR was not detected in the immunoprecipitate by anti-PTK7 antibody (Fig. 2A right panel). Moreover, in HEK293 cells ectopically expressing PTK7

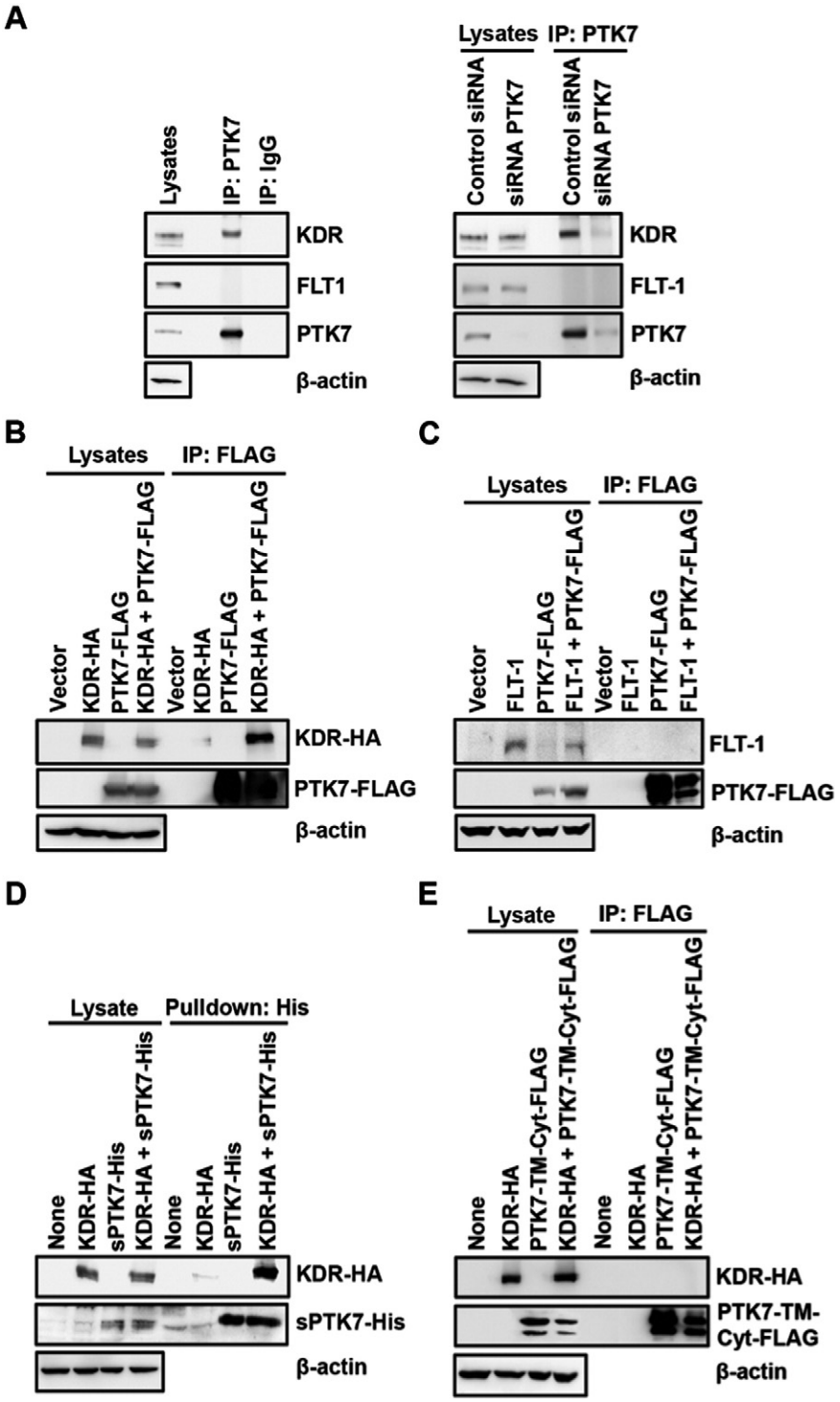

Fig. 2. Analysis of the interaction of PTK7 with VEGF receptors in HUVECs and HEK293 cells. (A) HUVECs (left panel) or HUVECs in which PTK7 was silenced by transfection of siRNAs (right panel) were lysed. Lysates were immunoprecipitated with anti-PTK7 antibody or IgG and protein-A Sepharose. (B, C) A PTK7-FLAG expression vector was transfected into HEK293 cells expressing KDR-HA (B) or FLT-1 (C). (D) HEK293 cells expressing KDR-HA were incubated with DMEM containing 53 nM sPTK7-His for 2 h at 4 °C. (E) An expression vector encoding PTK7-TM-Cyt-FLAG was transfected into HEK293 cells expressing KDR-HA. PTK7-FLAG (B, C) and PTK7-TM-Cyt-FLAG (E) were immunoprecipitated from the cell lysates with anti-FLAG antibody-conjugated agarose. sPTK7-His (D) was pulled down with Ni^{2+}-NTA agarose. Cell lysates (1/10 of lysates for HUVECs and 1/20 of lysates for HEK293 cells) and pulled-down proteins (9/10 of lysates for HUVECs and 19/20 of lysates for HEK293 cells) were subjected to SDS-PAGE and analyzed by immunoblotting with anti-KDR (A), anti-PTK7 (A), anti-FLT-1 (A, C), anti-HA (B, D), anti-penta-His (D), anti-FLAG (B, C, E), and anti-β-actin antibodies. Representative data from three independent experiments are shown.

and KDR or FLT-1, it was reproducible that FLAG-tagged PTK7 (PTK7-FLAG) was co-precipitated with HA-tagged KDR (KDR-HA) but not with FLT-1 (Fig. 2B and C).

To determine which domain of PTK7 interacts with KDR, HEK293 cells overexpressing KDR-HA were treated with purified His-tagged sPTK7 (sPTK7-His) or co-expressed with a FLAG-tagged PTK7 fragment containing the transmembrane and cytosolic domains (PTK7-TM-Cyt-FLAG). Pull-down assay showed that sPTK7 interacted with KDR (Fig. 2D) but transmembrane and cytosolic domains of PTK7 did not (Fig. 2E).

Binding specificity of PTK7 to KDR was further analyzed with purified extracellular domains of PTK7 (sPTK7), KDR (sKDR; 160 kDa), and FLT-1 (sFLT-1; 127 kDa) (Supplementary Fig. 1). sPTK7-His specifically bound to sKDR-Fc but not to sFLT-1-Fc when sPTK7-His was incubated with a mixture of sKDR-Fc and sFLT-1-Fc (Fig. 3).

3.3. A single sPTK7 molecule binds multiple molecules of KDR extracellular domain (sKDR) in vitro, and vice versa

To further characterize the interaction between sPTK7 and sKDR, the binding kinetics of sPTK7-His and sKDR-Fc were analyzed *in vitro*. Binding of sKDR-Fc to sPTK7-His (Fig. 4A) or of sPTK7-His to sKDR-Fc (Fig. 4B) was enhanced by increasing concentrations of sKDR-Fc and sPTK7-His, respectively. Saturation of the interactions was detected at input molar ratios of 1:8 and 8:1 of sPTK7 to sKDR. At saturation, the molar ratio of the bound molecule to the pulldown molecule was approximately 1:3, indicating that one molecule of sPTK7 binds to three molecules of sKDR, and *vice versa*.

3.4. sPTK7 modulates the interaction of sKDR and VEGF in vitro

To analyze the effect of sPTK7 on the VEGF–sKDR interaction, sKDR-Fc was preincubated with sPTK7 at molar ratios of 1:0, 1:0.25, 1:1, and 1:4, followed by incubation with increasing amounts of VEGF. Next, the amount of VEGF which co-precipitated with sKDR-Fc was determined.

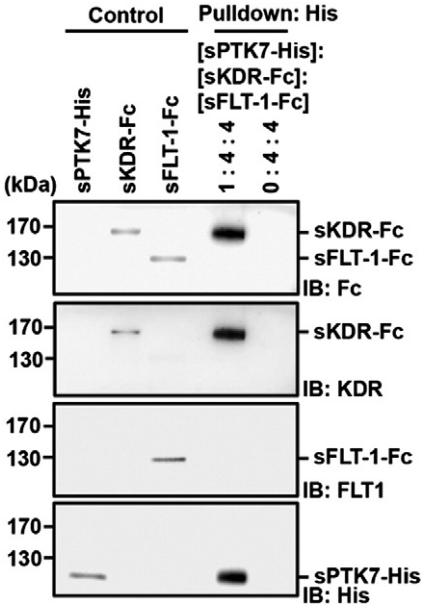

Fig. 3. Interaction of sPTK7 with extracellular domains of VEGF receptors *in vitro*. Purified sPTK7-His (2.5 pmol) was incubated with a mixture of sKDR-Fc (10 pmol) and sFLT-1-Fc (10 pmol) in 100 μl of a binding buffer (PBS containing 20 mM imidazole, 0.1% Triton X-100, and 0.01% BSA) for 2 h at 4 °C. Proteins pulled-down with Ni^{2+}-NTA agarose and controls (0.25 pmol each) were subjected to SDS-PAGE and analyzed by immunoblotting with anti-human Fc and anti-penta-His antibodies.

As expected, in the absence of sPTK7, increased VEGF concentrations resulted in increased VEGF–sKDR interaction (Fig. 5, [sPTK7]/[sKDR] = 0). Interestingly, preincubation of sKDR with sPTK7 at the 1:0.25 molar ratio enhanced VEGF–sKDR binding (Fig. 5, [sPTK7]/[sKDR] = 0.25). However, preincubation of sKDR with higher concentrations of sPTK7 (1:1 and 1:4 molar ratios) drastically decreased binding of VEGF to sKDR, (Fig. 5, [sPTK7]/[sKDR] = 1 and 4). Together with the data in the previous section (Fig. 4), these results show that when single molecules of sPTK7 bind several molecules of sKDR, the complexes bind more efficiently to VEGF than sPTK7-free sKDR. In contrast, when several molecules of sPTK7 bind to individual molecule of sKDR, the complexes bind less efficiently to VEGF.

3.5. sPTK7 modulates VEGF-induced KDR phosphorylation in HUVECs

sPTK7 is able to oligomerize sKDR and, at lower molar ratios to sKDR, enhances binding of VEGF to sKDR. However, at higher concentrations, it inhibits binding of VEGF to sKDR. In addition, we previously showed that treatment with a high concentration (53 nM; 4 μg/ml) of sPTK7 inhibited VEGF-induced physiological effects in HUVECs and angiogenesis *in vivo* [24]. To understand the effect of sPTK7 concentration on KDR activation, we analyzed VEGF-induced KDR phosphorylation in HUVECs in response to increasing amounts of sPTK7 (Fig. 6A). KDR phosphorylation levels gradually increased upon incubation of sPTK7 up to 0.5 nM, but, upon treatment with higher concentrations of sPTK7, decreased below the basal level without sPTK7 treatment. This pattern persisted when the experiment was replicated in HEK293 cells ectopically expressing KDR (Supplementary Fig. 3A and B left panel). On the other hand, as would be expected, phosphorylation of FLT-1 was not affected by increasing concentrations of sPTK7 (Supplementary Fig. 3A and B right panel).

The effect of sPTK7 on KDR phosphorylation was also analyzed in PTK7-knockdown HUVECs (Supplementary Fig. 4). Again, under these conditions, VEGF-induced KDR phosphorylation initially increased, and then decreased with increasing amounts of sPTK7 (Fig. 6B). In PTK7-knockdown HUVECs, however, the maximal effect was detected at 2 nM sPTK7, whereas the maximal effect was at 0.5 nM in PTK7-positive HUVECs. This was also the case with KDR-expressing HEK293 cells or PTK7-knockdown HEK293 cells (Supplementary Fig. 3B left panel and 3C). This result demonstrates that increasing concentrations of sPTK7 modulate VEGF-induced activation of KDR biphasically and suggests that a concentration of sPTK7 and/or PTK7 which induces the most efficient oligomerization of KDR molecules activates KDR maximally.

3.6. sPTK7 modulates VEGF-induced cell migration and in vivo angiogenesis

To observe whether modulation of KDR activation by sPTK7 led to changes in cell physiology, we analyzed the effect of sPTK7 on VEGF-induced migration of HUVECs (Fig. 6C). In this assay, cell migration was enhanced by increasing amounts of sPTK7, being highest in the presence of 0.5 nM sPTK7, and then decreased upon treatment with higher concentrations of sPTK7.

To examine whether increasing doses of sPTK7 affected angiogenesis *in vivo*, a Matrigel plug assay was performed in mice. To detect an increase in angiogenesis, we used a lower concentration (2.5 nM) of VEGF, compared with 10 nM in typical assays. After incubation in mice, plugs treated with VEGF alone were red-orange in color. Increasing concentrations of sPTK7 made the plugs darken in color up to 0.5 nM sPTK7, and then lighten with higher sPTK7 concentrations (Fig. 6D). Hemoglobin content also followed the same pattern (Fig. 6E). These results demonstrate that VEGF-induced cell migration and angiogenesis are also regulated biphasically in a sPTK7 concentration-dependent manner.

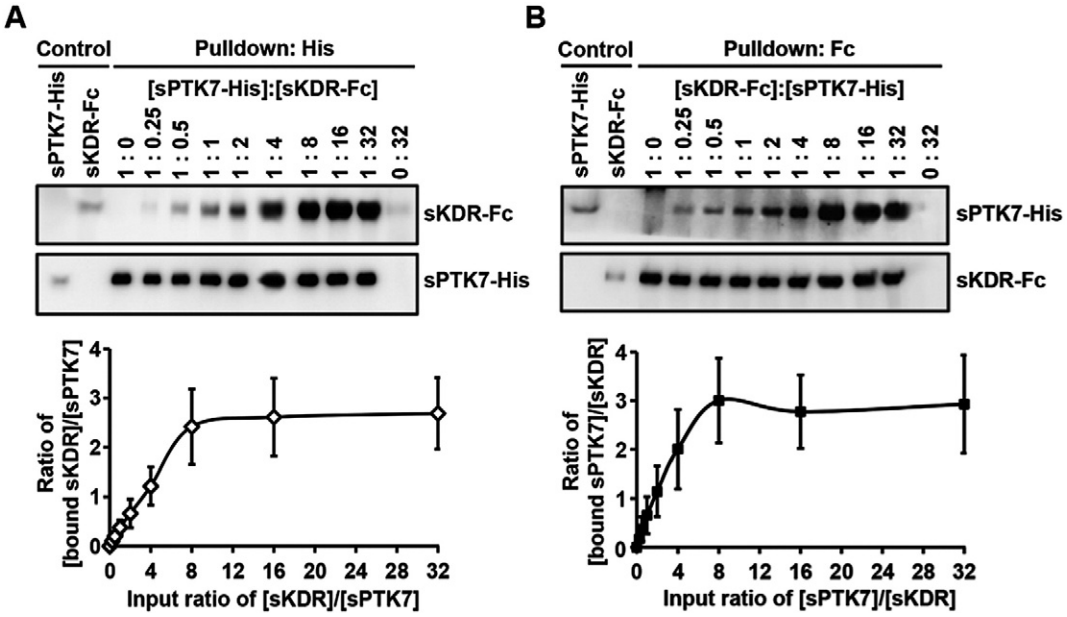

Fig. 4. Binding ratio of sPTK7 and sKDR *in vitro*. sPTK7-His (A) and sKDR-Fc (B) (2.5 pmol) were incubated with the indicated molar ratios of sKDR-Fc (A) and sPTK7-His (B), respectively, in 100 μl of the binding buffer for 2 h at 4 °C. Proteins pulled-down with Ni^{2+}-NTA agarose or protein-A Sepharose and controls (0.25 pmol each) were subjected to SDS-PAGE and analyzed by immunoblotting with anti-human Fc and anti-penta-His antibodies. Representative data from three independent experiments are shown. Protein amounts in the immunoblots were quantified by densitometry and were normalized with standard curves for sKDR-Fc and sPTK7-His. Graphs giving the relative ratios of [bound sKDR]/[sPTK7] or [bound sPTK7]/[sKDR] are shown below representative data.

3.7. VEGF-induced KDR-phosphorylation, migration, and capillary-like tube formation are controlled by the PTK7 expression level in HUVECs

Next, we analyzed whether VEGF-induced KDR-activation was modulated by expression of full-length PTK7, rather than treatment with sPTK7. To alter PTK7 expression levels in HUVECs, PTK7 was either gradually silenced by transfection with increasing amounts of PTK7 knockdown vector (pLKO.1-shRNA-PTK7) or gradually overexpressed by transfection with increasing amounts of PTK7 expression vector (pcDNA3-PTK7-FLAG). In response to increasing levels of PTK7 expression, VEGF-induced phosphorylation of KDR initially increased, and then decreased (Fig. 7A).

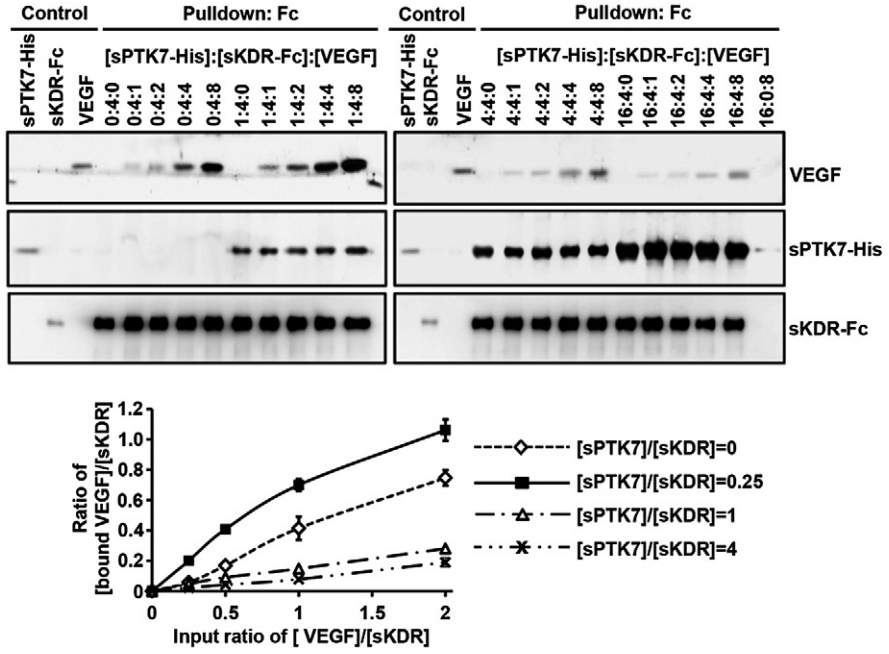

Fig. 5. Effect of sPTK7 on binding of VEGF to sKDR *in vitro*. sKDR-Fc (10 pmol) was pre-incubated with sPTK7-His (0, 2.5, 10, or 40 pmol) for 2 h, and the mixture was incubated with increasing amounts of VEGF (0, 2.5, 5, 10, or 20 pmol) in 100 μl of the binding buffer for 5 min at 4 °C with gentle agitation. Proteins pulled-down by protein-A Sepharose and controls (0.25 pmol each) were analyzed by immunoblotting with anti-human Fc, anti-penta-His, and anti-VEGF antibodies. Representative data from three independent experiments are shown. Amounts of proteins in the immunoblots were quantified by densitometry and normalized with standard curves for sKDR-Fc, sPTK7-His, and VEGF. The graph shows relative ratios of [bound VEGF]/[sKDR] *vs.* input ratios of [VEGF]/[sKDR]. Compared to determinants at [sPTK7]/[sKDR] = 0, all values were statistically significant ($P < 0.05$).

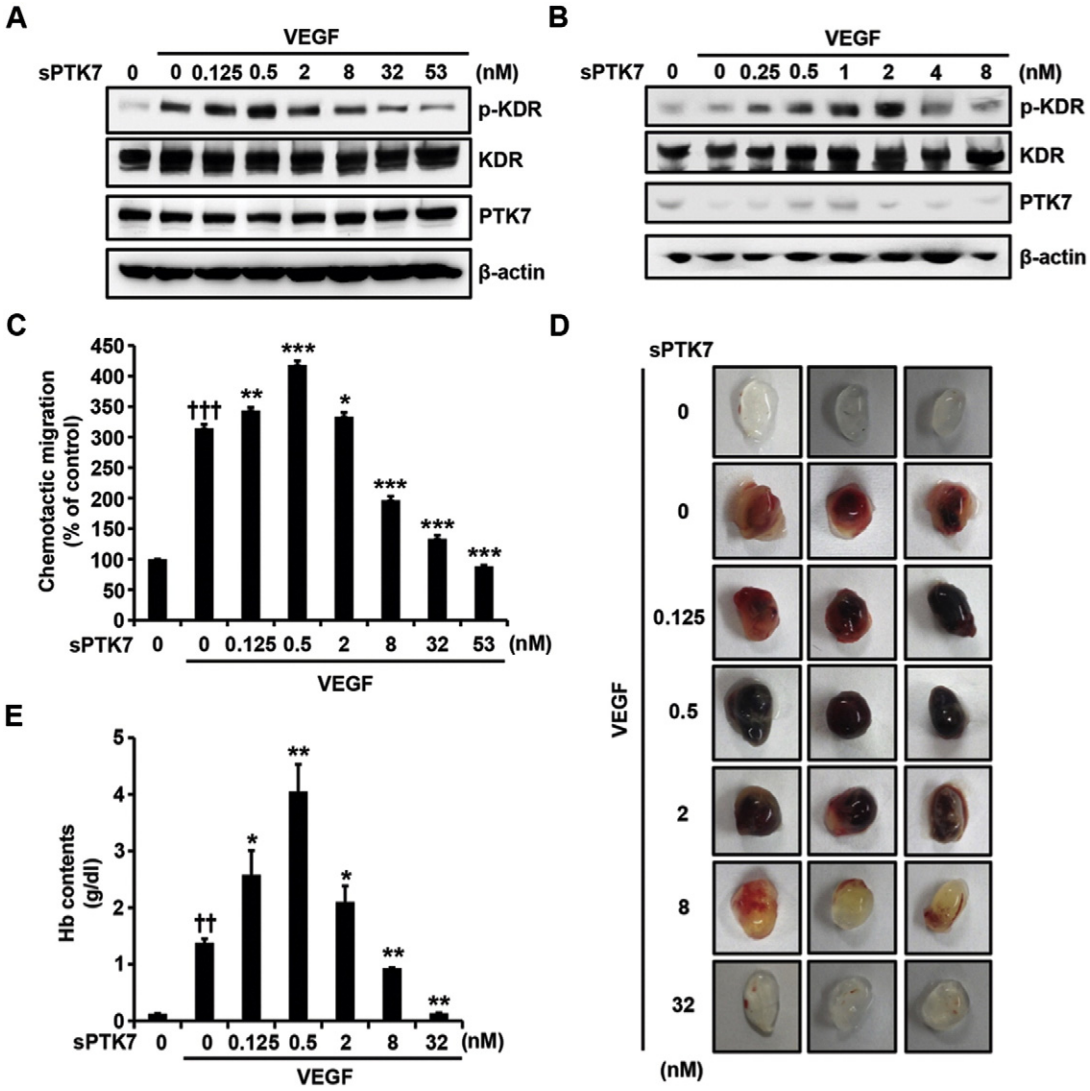

Fig. 6. Effect of increasing amounts of sPTK7 on VEGF-induced KDR phosphorylation and cell migration in HUVECs and angiogenesis in mice. (A, B) HUVECs were transfected with a control vector (A) or a PTK7 knockdown vector (B). The HUVECs were starved in a medium containing 1% FBS for 6 h. They were preincubated with the indicated amounts of sPTK7 for 30 min at 37 °C, and then stimulated with VEGF for 5 min. Phosphorylation of KDR was analyzed by immunoblotting with anti-phospho-KDR (Y951), anti-KDR, anti-PTK7, and anti-β-actin antibodies. (C) Starved HUVECs were detached with trypsin and incubated with the indicated amounts of sPTK7 for 30 min. VEGF-induced chemotactic migration of the cells was analyzed using a Transwell chamber (n = 3). (D, E) Matrigel was mixed with 16 units of heparin, and either 2.5 nM mouse VEGF or VEGF plus the indicated amounts of mouse sPTK7, and injected into the abdomens of mice subcutaneously (3 plugs per group). After 9 days, the plugs were recovered. Representative images of the Matrigel plugs (D) and measurements of hemoglobin content in the Matrigel plugs (E) are shown. $^{\dagger\dagger}P < 0.01$ and $^{\dagger\dagger\dagger}P < 0.001$ *vs.* non-VEGF-treated control, $^{*}P < 0.05$, $^{**}P < 0.01$, and $^{***}P < 0.001$ *vs.* a sample treated with VEGF alone.

In addition, we analyzed the effect of PTK7 levels on migration and capillary-like tube formation of HUVECs. In agreement with the pattern of VEGF-induced KDR phosphorylation, increasing amounts of PTK7 first increased and then decreased both cell migration (Fig. 7B) and tube formation (Fig. 7C and D). The highest levels of cell migration and tube formation, as well as of KDR phosphorylation, were achieved when HUVECs were transfected with 1 μg of PTK7 expression vector.

4. Discussion

We previously showed that treatment of HUVECs with a high dose of sPTK7 (6.25 to 53 nM) inhibited VEGF-induced migration, invasion, and tube formation in a dose-dependent manner [24]. Dana and colleagues reported that PTK7 knockdown inhibited VEGF-induced phosphorylation of FLT-1, but not KDR, in mouse endothelial MS1 cells and that PTK7 interacted with FLT-1, but not with KDR or FLT-4 [26]. In contrast, we found that treatment of HUVECs with a high dose of sPTK7 (53 nM) or knockdown of PTK7 inhibited VEGF-induced phosphorylation of KDR, but not FLT-1. In HUVECs and HEK293 cells expressing PTK7 and a specific RPTK, KDR co-precipitated with PTK7, but FLT-1 did not. Moreover, we demonstrated that PTK7 and KDR interacted through their extracellular domains *in vitro* and in cells. Therefore, PTK7 plays a role in angiogenesis by controlling activation of KDR.

Terman and colleagues found that deletion of the 4th to 7th immunoglobulin domains of KDR led to VEGF-independent receptor activation [27]. Ballmer-Hofer and colleagues reported that the affinity of $VEGF_{165}$ for sKDR was 6–21-fold lower than for the 2nd and 3rd immunoglobulin domains of KDR, as assessed by thermodynamic analysis [28]. These results suggest that the presence of the 4th to 7th immunoglobulin domains of KDR inhibits ligand-independent KDR dimerization and kinase activation. In fact, negative-staining electron microscopy revealed that ligand-free sKDR molecules are present as flexible monomers [29]. Interestingly, we found above using an *in vitro* binding assay that sPTK7 could form ligand-free hetero-oligomers with sKDR. Maximally, 2.76 sKDR molecules interacted with a single PTK7 molecule at a molar ratio of sPTK7 to sKDR higher than 1:8. In serum-depleted HUVECs, the molar ratio of PTK7 to KDR is 1:3.6 (13.0×10^{-18} mol of PTK7 molecules and 46.6×10^{-18} mol of KDR molecules per cell)

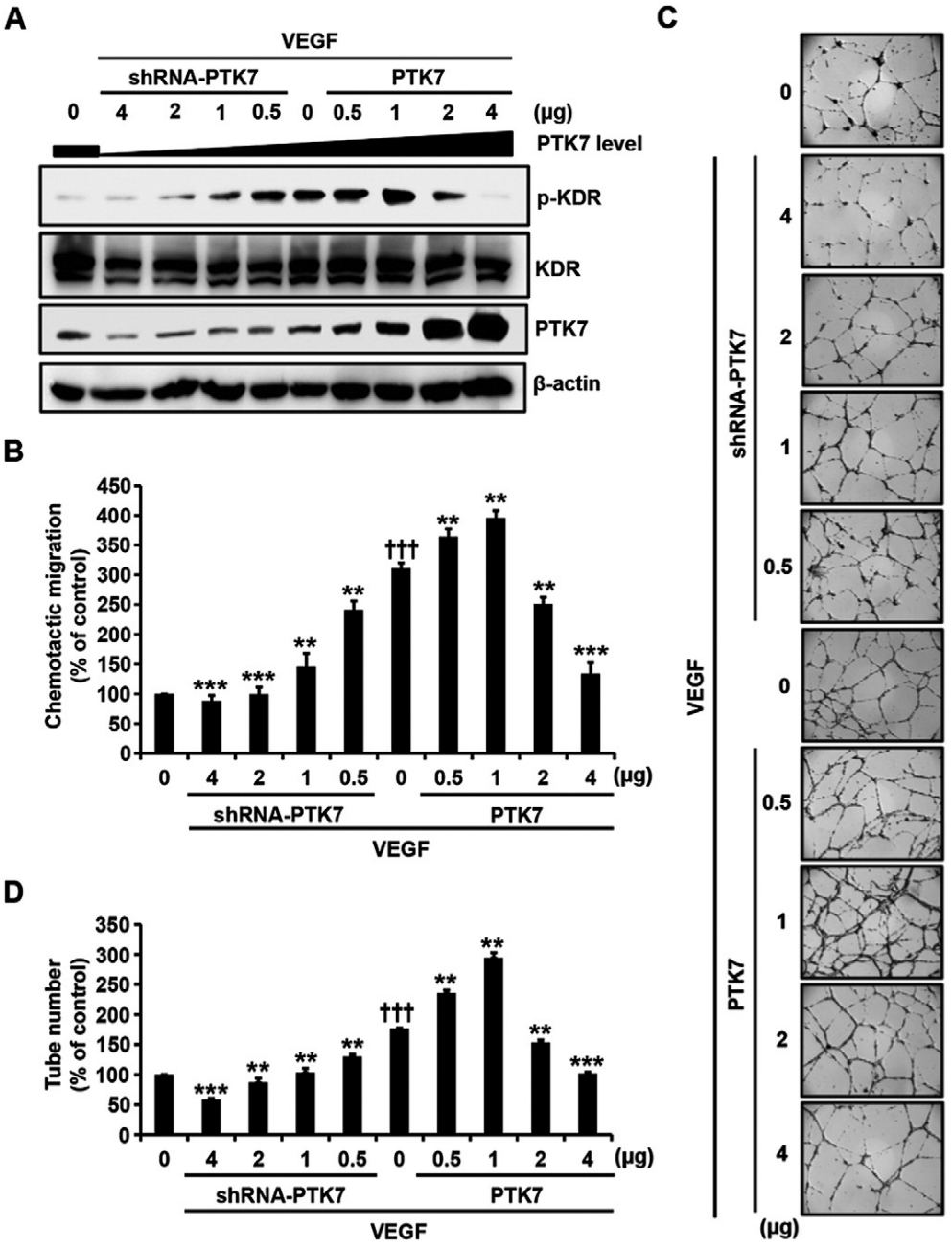

Fig. 7. Effect of increasing levels of PTK7 expression on VEGF-induced KDR phosphorylation, cell migration, and capillary-like tube formation in HUVECs. HUVECs were transfected with increasing amounts of PTK7 knockdown vector (pLKO.1-shRNA-PTK7-6434; shRNA-PTK7) or PTK7 expression vector (pcDNA3-PTK7-FLAG; PTK7). After 48 h, the HUVECs were starved in a medium containing 1% FBS for 6 h. (A) The cells were stimulated with 0.5 nM VEGF for 5 min, and the phosphorylation of KDR was examined by immunoblotting using anti-phospho-KDR (Y951), anti-KDR, anti-PTK7, and anti-β-actin antibodies. (B, C, D) The cells were detached and subjected to a VEGF-induced chemotactic migration assay (B) or a capillary-like tube formation assay (C) as described previously [24]. Representative light micrographs of the capillary-like tube formation assay are shown in (C) (Magnification, 60×). Tube numbers in (C) were counted and plotted in (D). $^{\dagger\dagger\dagger}P < 0.001$ *vs.* non-VEGF-treated control, $^{**}P < 0.01$, $^{***}P < 0.001$ *vs.* HUVECs treated with VEGF alone.

(Supplementary Fig. 5). Based on this, we propose that PTK7 can stimulate ligand-free oligomerization of KDR molecules on the cell surface.

In addition to the role of PTK7 in KDR oligomerization, the presence of sPTK7 at molar ratios lower than sKDR (for example, 0.25:1 input molar ratio of sPTK7 to sKDR) enhanced binding of VEGF to sKDR, compared with the absence of sPTK7. Since VEGF did not bind to sPTK7 (Supplementary Fig. 6), we suggest that sKDR bound to sPTK7 has a higher affinity for VEGF due to a conformational change. In contrast, at higher levels of PTK7 (higher than 1:8 molar ratios of sKDR to sPTK7), one sKDR molecule can form hetero-oligomers involving up to three sPTK7 molecules. In addition, when sPTK7 was present at the same or a higher molar concentration than sKDR, the enhancement of VEGF–sKDR binding by sPTK7 was diminished.

Based on our findings, we propose a model for the role of PTK7 in modulating KDR activation (Fig. 8). At lower molar ratios, PTK7 enhances KDR signaling by oligomerization of KDR and this increases binding of VEGF to the KDR oligomers. The increased VEGF–KDR binding is probably due to a PTK7-induced conformational change of KDR that increases its affinity for VEGF and/or to increased local concentrations of KDR resulting from its hetero-oligomerization. Conversely, at higher molar ratios, PTK7 inhibits activation of KDR because the KDR molecules are enclosed by PTK7 molecules and, therefore, cannot bind

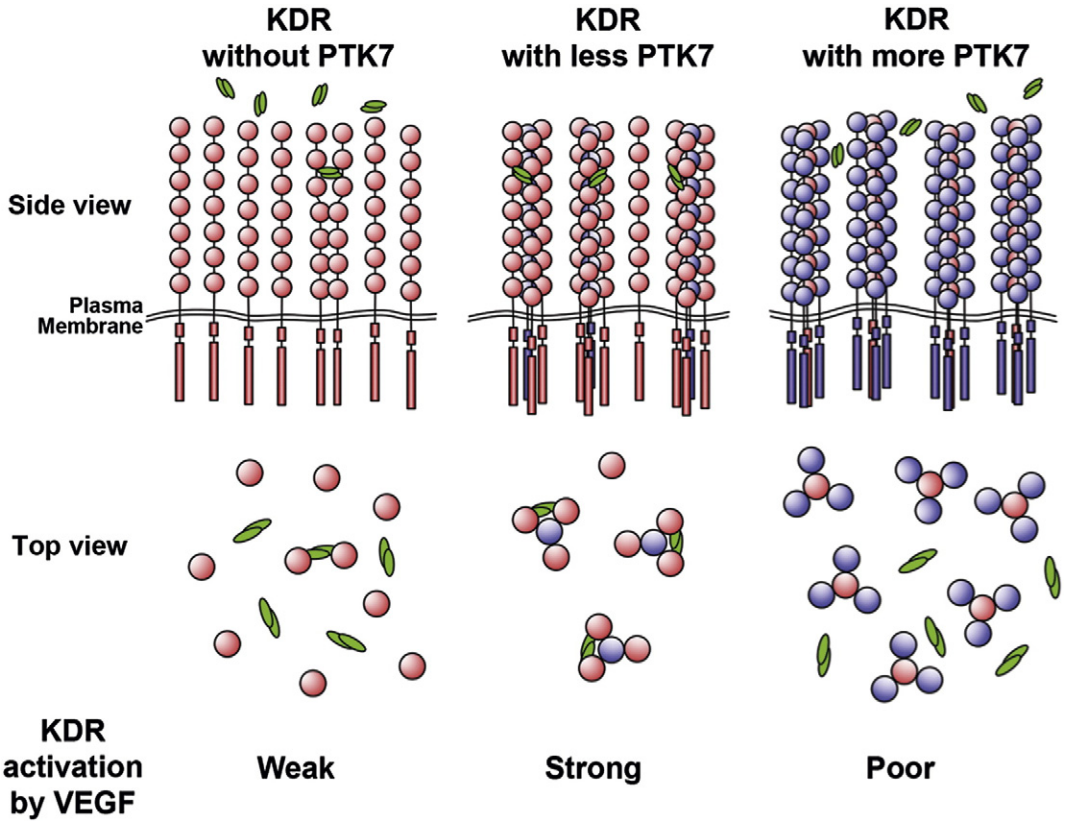

Fig. 8. A model for the modulation of KDR activity *via* PTK7. In the absence of PTK7 (blue), KDR molecules (red) can be dimerized and activated by VEGF dimers (green). In the presence of PTK7 at concentrations lower than the KDR concentration, one PTK7 molecule can bind together up to three ligand-free KDR molecules. Due to a PTK7-mediated conformational change and/or the increased local concentrations of KDR molecules, the PTK7-bound KDR molecules readily bind to the VEGF dimers and are activated. However, when PTK7 is present at much higher concentrations than KDR, each KDR molecule is enclosed by several PTK7 molecules and cannot bind to the VEGF dimers. Overall, increasing levels of PTK7 thus result in an up-and-down biphasic pattern of modulation of VEGF-induced KDR activation.

efficiently to VEGF. This mechanism for PTK7-induced KDR activation is similar to a previously proposed model for increased MAPK activation by a scaffold protein [30]. In the model, at lower concentrations, the scaffold protein recruits signaling components and increases output signaling. However, at higher concentrations, scaffold proteins separate the signaling components, inhibiting the signaling cascade. In both models, the optimal concentration of PTK7 or scaffold protein is important for maximal activation of signaling partners.

We hypothesized that increasing expression levels of PTK7 would show an up-and-down biphasic pattern for VEGF-induced KDR activation *in vivo*. As expected, we found that increasing concentrations of sPTK7 initially increases KDR activation in HUVECs, followed by a decrease. In normal HUVECs, 0.5 nM sPTK7 maximally activates the VEGF-induced KDR phosphorylation. In HUVECs where PTK7 has been knocked down, the maximal activation of VEGF-induced KDR phosphorylation requires a higher concentration of sPTK7 (2 nM). This result suggests that the endogenous PTK7 level in HUVECs is sub-optimal (approximately 75%) for maximal KDR activation. The effect of sPTK7 on VEGF-induced signaling was also seen in endothelial cells examined in an *in vivo* angiogenesis assay. Moreover, our experiments exposing HUVECs to a range of full-length PTK7 levels clearly demonstrated that PTK7 modulated VEGF-induced physiological events, such as KDR activation, chemotactic migration, and capillary-like tube formation of HUVECs with a bell-shaped dose response curve.

We and others have shown that knockdown of PTK7 decreases proliferation, survival, wound healing, and invasion of esophageal squamous cell carcinoma cells [20] and reduces cell viability and tumor burden in lung adenocarcinoma [31], demonstrating oncogenic roles for PTK7. In contrast, we also noted a tumor-suppressive role of PTK7, as overexpression of PTK7 decreased cell proliferation, invasion, and migration in lung squamous cell carcinoma [32]. These findings can be explained with our model for a biphasic effect of PTK7 on RPTK activity, because knockdown and overexpression of PTK7 would represent extremes of the bell-shaped PTK7 dose–response curve.

5. Conclusions

Our results suggest a novel mechanism for the biphasic regulation of KDR activity by PTK7: at lower concentrations, PTK7 activates KDR by promoting KDR oligomerization and so increasing its affinity for the ligand, and at higher concentrations, PTK7 inhibits the pathway by surrounding KDR. Our findings concerning the role of PTK7 in activation of KDR should contribute to controlling diseases involving KDR, such as pathological angiogenesis.

Transparency document

The Transparency document associated with this article can be found in the online version.

Acknowledgements

This work was supported by grants from the National Research Foundation of Korea (No. 2012R1A1A2007638 and No. 2013R1A2A2A01013884). W.S.S. was a recipient of the postdoctoral trainee program of the Yonsei University Research Fund.

Appendix A. Supplementary data

Supplementary data to this article can be found online at http://dx.doi.org/10.1016/j.bbamcr.2015.05.015.

References

[1] J.M. Mendrola, F. Shi, J.H. Park, M.A. Lemmon, Receptor tyrosine kinases with intracellular pseudokinase domains, Biochem. Soc. Trans. 41 (2013) 1029–1036.
[2] T. Holbro, R.R. Beerli, F. Maurer, M. Koziczak, C.F. Barbas III, N.E. Hynes, The ErbB2/ErbB3 heterodimer functions as an oncogenic unit: ErbB2 requires ErbB3 to drive breast tumor cell proliferation, Proc. Natl. Acad. Sci. U. S. A. 100 (2003) 8933–8938.
[3] C.L. Arteaga, J.A. Engelman, ERBB receptors: from oncogene discovery to basic science to mechanism-based cancer therapeutics, Cancer Cell 25 (2014) 282–303.
[4] M.M. Halford, J. Armes, M. Buchert, V. Meskenaite, D. Grail, M.L. Hibbs, A.F. Wilks, P.G. Farlie, D.F. Newgreen, C.M. Hovens, S.A. Stacker, Ryk-deficient mice exhibit craniofacial defects associated with perturbed Eph receptor crosstalk, Nat. Genet. 25 (2000) 414–418.
[5] K. Kamitori, M. Tanaka, T. Okuno-Hirasawa, S. Kohsaka, Receptor related to tyrosine kinase RYK regulates cell migration during cortical development, Biochem. Biophys. Res. Commun. 330 (2005) 446–453.
[6] L. Truitt, A. Freywald, Dancing with the dead: Eph receptors and their kinase-null partners, Biochem. Cell Biol. 89 (2011) 115–129.
[7] W. Lu, V. Yamamoto, B. Ortega, D. Baltimore, Mammalian Ryk is a Wnt coreceptor required for stimulation of neurite outgrowth, Cell 119 (2004) 97–108.
[8] J. Green, R. Nusse, R. van Amerongen, The role of Ryk and Ror receptor tyrosine kinases in Wnt signal transduction, Cold Spring Harb. Perspect. Biol. 6 (2014) a009175.
[9] S.T. Lee, K.M. Strunk, R.A. Spritz, A survey of protein tyrosine kinase mRNAs expressed in normal human melanocytes, Oncogene 8 (1993) 3403–3410.
[10] S.K. Park, H.S. Lee, S.T. Lee, Characterization of the human full-length PTK7 cDNA encoding a receptor protein tyrosine kinase-like molecule closely related to chick KLG, J. Biochem. 119 (1996) 235–239.
[11] J.W. Jung, W.S. Shin, J. Song, S.T. Lee, Cloning and characterization of the full-length mouse Ptk7 cDNA encoding a defective receptor protein tyrosine kinase, Gene 328 (2004) 75–84.
[12] J.M. Murphy, Q. Zhang, S.N. Young, M.L. Reese, F.P. Bailey, P.A. Eyers, D. Ungureanu, H. Hammaren, O. Silvennoinen, L.N. Varghese, K. Chen, A. Tripaydonis, N. Jura, K. Fukuda, J. Qin, Z. Nimchuk, M.B. Mudgett, S. Elowe, C.L. Gee, L. Liu, R.J. Daly, G. Manning, J.J. Babon, I.S. Lucet, A robust methodology to subclassify pseudokinases based on their nucleotide-binding properties, Biochem. J. 457 (2014) 323–334.
[13] M.L. Winberg, L. Tamagnone, J. Bai, P.M. Comoglio, D. Montell, C.S. Goodman, The transmembrane protein Off-track associates with Plexins and functions downstream of Semaphorin signaling during axon guidance, Neuron 32 (2001) 53–62.
[14] T. Toyofuku, H. Zhang, A. Kumanogoh, N. Takegahara, F. Suto, J. Kamei, K. Aoki, M. Yabuki, M. Hori, H. Fujisawa, H. Kikutani, Dual roles of Sema6D in cardiac morphogenesis through region-specific association of its receptor, Plexin-A1, with off-track and vascular endothelial growth factor receptor type 2, Genes Dev. 18 (2004) 435–447.
[15] X. Lu, A.G. Borchers, C. Jolicoeur, H. Rayburn, J.C. Baker, M. Tessier-Lavigne, PTK7/CCK-4 is a novel regulator of planar cell polarity in vertebrates, Nature 430 (2004) 93–98.
[16] F. Puppo, V. Thome, A.C. Lhoumeau, M. Cibois, A. Gangar, F. Lembo, E. Belotti, S. Marchetto, P. Lecine, T. Prebet, M. Sebbagh, W.S. Shin, S.T. Lee, L. Kodjabachian, J.P. Borg, Protein tyrosine kinase 7 has a conserved role in Wnt/beta-catenin canonical signalling, EMBO Rep. 12 (2011) 43–49.
[17] N. Bin-Nun, H. Lichtig, A. Malyarova, M. Levy, S. Elias, D. Frank, PTK7 modulates Wnt signaling activity via LRP6, Development 141 (2014) 410–421.
[18] K. Mossie, B. Jallal, F. Alves, I. Sures, G.D. Plowman, A. Ullrich, Colon carcinoma kinase-4 defines a new subclass of the receptor tyrosine kinase family, Oncogene 11 (1995) 2179–2184.
[19] S. Saha, A. Bardelli, P. Buckhaults, V.E. Velculescu, C. Rago, B. St Croix, K.E. Romans, M.A. Choti, C. Lengauer, K.W. Kinzler, B. Vogelstein, A phosphatase associated with metastasis of colorectal cancer, Science 294 (2001) 1343–1346.
[20] W.S. Shin, J. Kwon, H.W. Lee, M.C. Kang, H.W. Na, S.T. Lee, J.H. Park, Oncogenic role of protein tyrosine kinase 7 in esophageal squamous cell carcinoma, Cancer Sci. 104 (2013) 1120–1126.
[21] D.J. Easty, P.J. Mitchell, K. Patel, V.A. Florenes, R.A. Spritz, D.C. Bennett, Loss of expression of receptor tyrosine kinase family genes PTK7 and SEK in metastatic melanoma, Int. J. Cancer 71 (1997) 1061–1065.
[22] H. Wang, G. Li, Y. Yin, J. Wang, H. Wang, W. Wei, Q. Guo, H. Ma, Q. Shi, X. Zhou, J. Wang, PTK7 protein is decreased in epithelial ovarian carcinomas with poor prognosis, Int. J. Clin. Exp. Pathol. 7 (2014) 7881–7889.
[23] H.W. Na, W.S. Shin, A. Ludwig, S.T. Lee, The cytosolic domain of PTK7, generated from sequential cleavage by ADAM17 and gamma-secretase, enhances cell proliferation and migration in colon cancer cells, J. Biol. Chem. 287 (2012) 25001–25009.
[24] W.S. Shin, Y.S. Maeng, J.W. Jung, J.K. Min, Y.G. Kwon, S.T. Lee, Soluble PTK7 inhibits tube formation, migration, and invasion of endothelial cells and angiogenesis, Biochem. Biophys. Res. Commun. 371 (2008) 793–798.
[25] M. Wigler, R. Sweet, G.K. Sim, B. Wold, A. Pellicer, E. Lacy, T. Maniatis, S. Silverstein, R. Axel, Transformation of mammalian cells with genes from prokaryotes and eukaryotes, Biotechnology 24 (1992) 444–452.
[26] H.K. Lee, S.K. Chauhan, E. Kay, R. Dana, Flt-1 regulates vascular endothelial cell migration via a protein tyrosine kinase-7-dependent pathway, Blood 117 (2011) 5762–5771.
[27] Q. Tao, M.V. Backer, J.M. Backer, B.I. Terman, Kinase insert domain receptor (KDR) extracellular immunoglobulin-like domains 4–7 contain structural features that block receptor dimerization and vascular endothelial growth factor-induced signaling, J. Biol. Chem. 276 (2001) 21916–21923.
[28] M.S. Brozzo, S. Bjelic, K. Kisko, T. Schleier, V.M. Leppanen, K. Alitalo, F.K. Winkler, K. Ballmer-Hofer, Thermodynamic and structural description of allosterically regulated VEGFR-2 dimerization, Blood 119 (2012) 1781–1788.
[29] C. Ruch, G. Skiniotis, M.O. Steinmetz, T. Walz, K. Ballmer-Hofer, Structure of a VEGF–VEGF receptor complex determined by electron microscopy, Nat. Struct. Mol. Biol. 14 (2007) 249–250.
[30] A. Levchenko, J. Bruck, P.W. Sternberg, Scaffold proteins may biphasically affect the levels of mitogen-activated protein kinase signaling and reduce its threshold properties, Proc. Natl. Acad. Sci. U. S. A. 97 (2000) 5818–5823.
[31] R. Chen, P. Khatri, P.K. Mazur, M. Polin, Y. Zheng, D. Vaka, C.D. Hoang, J. Shrager, Y. Xu, S. Vicent, A.J. Butte, E.A. Sweet-Cordero, A meta-analysis of lung cancer gene expression identifies PTK7 as a survival gene in lung adenocarcinoma, Cancer Res. 74 (2014) 2892–2902.
[32] J.H. Kim, J. Kwon, H.W. Lee, M.C. Kang, H.J. Yoon, S.T. Lee, J.H. Park, Protein tyrosine kinase 7 plays a tumor suppressor role by inhibiting ERK and AKT phosphorylation in lung cancer, Oncol. Rep. 31 (2014) 2708–2712.